

RANGE AND RESTRICTED ENERGY-LOSS DATA FOR LIGHT AND HEAVY IONS IN PM-555 AND METAPHOSPHATE GLASSES NUCLEAR TRACK DETECTORS

Moustafa H. Aly

Department of Engineering Mathematics and Physics,
Faculty of Engineering, Alexandria University,
Alexandria, Egypt.

A. Abdel-Naby

Department of Physics and Chemistry,
Faculty of Education, Alexandria University,
Alexandria, Egypt.

ABSTRACT

Range-energy and restricted energy loss (REL) data are calculated for light and heavy ions over the energy interval 0.0025-20 MeV/nucl. in PM-555 produced from diethyleneglycol bis (allylcarbonate) and metaphosphate glass nuclear track detectors, which are extensively used in many applications. The method used to generate the range and REL data in any stopping material of known composition is briefly outlined. The calculations are based on one of the popular semiempirical formalism used for the analysis of nuclear tracks in solids.

INTRODUCTION

Solid state nuclear track detectors (SSNTDs) possess a number of advantages over rival dosimeters. These include: i) cheapness of the plastic detecting-foils, ii) compact geometry which under certain circumstances gives them an overwhelming advantage over electronic devices, iii) ease of development, iv) permanence of record and v) selectivity of response [1]. The knowledge of the range-energy is essential for the investigation of the properties of these detectors since: i) the energy loss rate (dE/dx) plays a critical role in particle registration efficiency and ii) the length of tracks and location of maximum energy deposition are dependent upon the range of particles. The knowledge of the energy loss, responsible for the etchable nuclear tracks and of the range-energy relation of nuclear particles, is an essential requirement in almost all fields when any nuclear track detector is used.

To face this need, the computer program of Henke and Benton [2] is provided to calculate the range and energy-loss rate of a charged particle travelling through any given medium, as a function of four parameters of the incident ion: i) the atomic mass number per electron (A/Z), ii) the mean ionization energy (I) of the stopping material (which may be the track detector), iii) the atomic number and iv) the energy per nucleon.

In the present work, computed range and REL data are given for some representative light and heavy ions over an energy interval 0.0025-20 MeV/nucl., in which studies are frequently performed when polymeric and glassy nuclear

track detectors are used. The data are computed for the chemical composition related to the PM-555 and metaphosphate glass ZnP nuclear track detectors. The urgent need of range-energy and REL data is particularly true in the case of PM-555 track detectors of unique sensitivity which are efficiently utilized in more and more applications. The data computed for the REL are listed for some representative ions: $\{^1\text{H}, ^4\text{He}, ^{12}\text{C}, ^{16}\text{O}, ^{20}\text{Ne}, ^{56}\text{Fe}, ^{235}\text{U}$ and $^{238}\text{U}\}$ for the PM-555 and $\{^4\text{He}, ^{12}\text{C}, ^{16}\text{O}, ^{20}\text{Ne}, ^{56}\text{Fe}, ^{235}\text{U}$ and $^{238}\text{U}\}$ for the metaphosphate glass. This may be reasonably used in determining the response registration function of polymeric and glassy nuclear track detectors. The REL data are given at different values for the upper limit of the δ -ray energy, ω_0 , in the composition between 0.1 and 1 keV. These may help to find the best response curve for PM-555 and metaphosphate glass to find high resolution with different nuclear charge and energy.

THEORY AND METHOD

A. The Range Calculations

The range calculations are based on a semiempirical theoretical model presented by Barkas and Berger [3], modified and extended by Henke and Benton [4]. The uncertainty in the range data obtained by such a calculation formalism, according to the independent set of

measurements performed in the energy interval 1-10 MeV/nucl., is smaller than 2%. When using this calculation method, the range of different ions at a given velocity $v = \beta c$, can be derived from the relationship [5]:

$$R(\beta) = M [\lambda(\beta) + B_z(\beta)]/z^2, \quad (1)$$

where $\lambda(\beta)$ is the range of an ideal proton (i.e. a proton with no charge neutralization near the stopping end of the trajectory), $B_z(\beta)$ is the generalized range extension caused by the charge neutralization as the ion comes to rest, M and z are the mass and charge of the ion. The expressions for $\lambda(\beta)$ and $B_z(\beta)$ can be computed from the Benton equations [5].

B. The REL Calculations

In polymeric and glassy track detectors, the restricted energy loss (REL) has proved to be sufficiently good to characterize the etching behavior of the damaged zones produced along nuclear tracks. In this model, it is assumed that only knock-on electrons with energy smaller than a given maximum value, ω_o , can play dominant role in causing etchable radiation damages. In the model, ω_o is the upper limit of the δ -ray energy in the composition, and is considered as a fitting parameter.

In the present work, for the calculation of REL (ω_o) values, we have used the formula of Somogyi et al. [6], as follows:

$$REL = REL1 = z^2 \{ \lambda(\beta) + B_z(\beta) (1 - \beta^2)^{3/2} / (931.141 \beta) \}^{-1} \text{ if } \Delta_1 \leq 0 \quad (2-a)$$

$$= REL2 = REL1 - \Delta_1 \text{ if } \Delta_1 \geq 0 \quad (2-b)$$

$$= REL3 = REL1 - REL2 + \Delta_2 \text{ if } \Delta_1 + \Delta_2 \leq REL2, \quad (2-c)$$

where $\lambda(\beta)$ and $B_z(\beta)$ can be computed using Benton equations [5], Δ_1 and Δ_2 are given by:

$$\Delta_1 = K n z^2_{eff} \beta^{-2} \{ \ln(\omega_m/\omega_o) - \beta^2 \}, \quad (3-a)$$

and

$$\Delta_2 = 2K n z^2_{eff} \beta^{-2} \{ \ln(\omega_o/I_c) - C(\beta) \}, \quad (3-b)$$

where

$$K = 2\pi e^4/m_e c^2 = 2.55 \times 10^{-25} \text{ MeV.cm}^2, \quad (4-a)$$

$$n = \rho N_A/(A/Z) \text{ electron.cm}^{-3}, \quad (4-b)$$

$$z_{eff} = z \{ 1 - \exp(-125 \beta/z^{2/3}) \}, \quad (4-c)$$

$$\beta^2 = 1 - \{ 1 + (E/931.141 M) \}^{-2}, \quad (4-d)$$

$$\omega_m = 2\pi c^2 \beta^2 (1 - \beta^2)^{-1}, \quad (4-e)$$

$$\ln I_c = (A/Z) \sum_i f_i \langle Z/A \rangle_i \ln I_i, \quad (4-f)$$

$$I_i(\text{eV}) = \begin{cases} 12 Z_i + 7 & \text{if } Z_i \leq 13 \\ 9.76 Z_i + 58.8 Z_i^{-0.19} & \text{if } Z_i \geq 13 \end{cases}, \quad (4-g)$$

$$f_i = \frac{\mu_i A_i}{\sum_j \mu_j A_j}, \quad (4-h)$$

$$(A/Z)^{-1} = \sum_i f_i (Z/A), \quad (4-i)$$

$$C(\beta) = (A/Z) \sum_i \frac{f_i C_i}{A_i}, \quad (4-j)$$

$$C_i = \sum_{m=2} \sum_{n=1} a_{mn} (\beta^{-2} - 1)^n I_i^m, \quad (4-k)$$

with

- z, M, E : the charge, mass and energy of the ion,
- μ_i : number of the i th component in the chemical formula of the stopping material,
- Z_i, A_i : atomic numbers and atomic weights in the stopping material,
- a_{mn} : a parameter given by Barkas and Berger [3],
- and
- ρ : density of the stopping material.

RESULTS AND DISCUSSION

Equation (1) is used to calculate the range energy. The variation of the range energy with the particle energy for different ions is displayed in Figures (1 and 2) for the polymer PM-555 and the metaphosphate glass, respectively. From these figures, it is clear that the range energy increases with the ion energy.

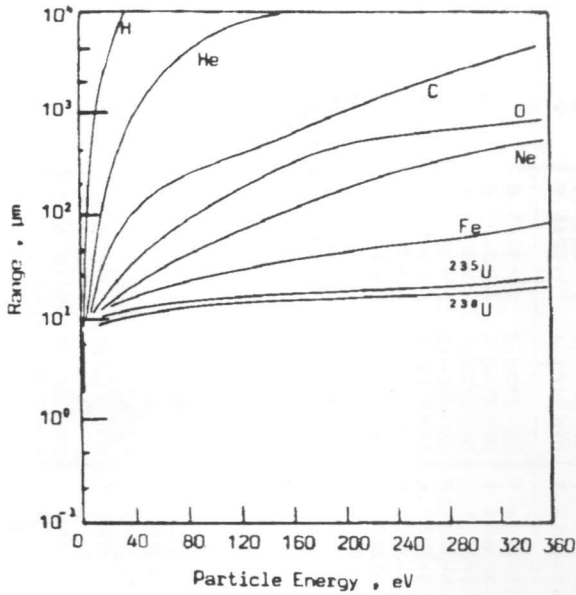


Figure 1. Variation of the range with particle energy in PM-555 for different ions.

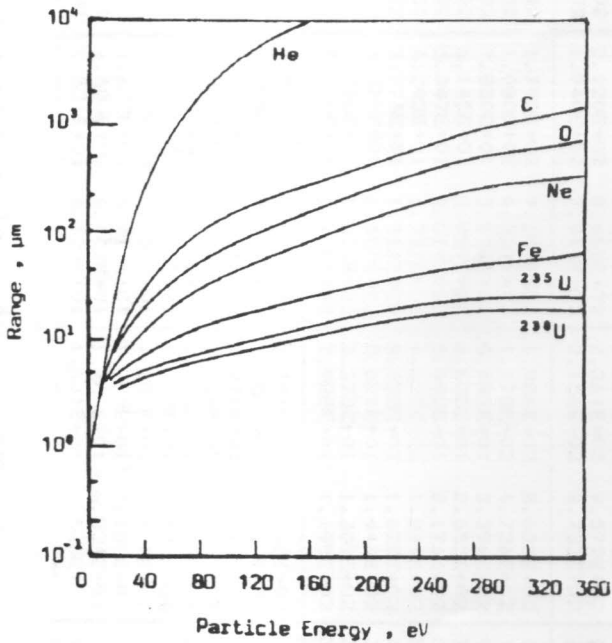


Figure 2. Variation of the range with particle energy in metaphosphate glass for different ions.

The restricted energy loss REL is computed through equations (2 - a, b and c) at $\omega_0 = 300$ eV for certain ions. A sample of the obtained results is shown in Figure (3), for the ^4He ion in both materials. The main features of the variation of the REL with the particle energy, shown

in Figure (3), are exactly the same for all considered ions. This result is in consistence with the Bragg curve [7]. Here, one must keep in mind that, we have used, in a new trend, the effective charge z_{eff} , equation (4-c), instead of the charge z . The effect of the upper limit of the δ -ray energy, ω_0 , on the REL is also studied in the interval 0.1-1 keV.

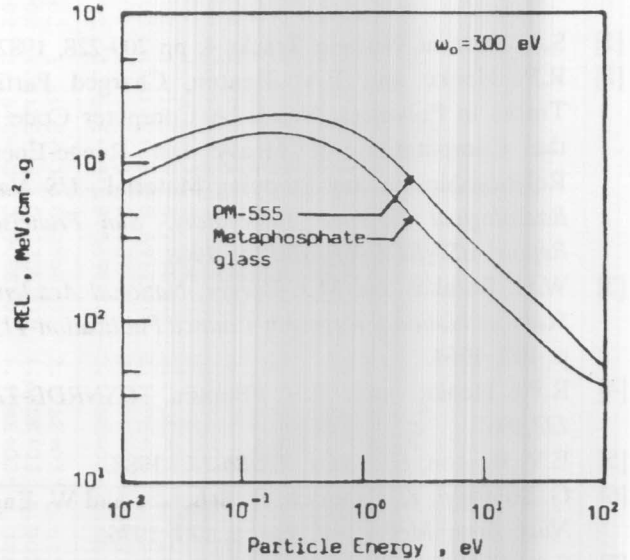


Figure 3. Variation of REL with particle energy for the He ion.

In most cases when the nuclear track detectors are investigated, it is preferable to list the data in tables giving the accurate values of the REL in order to choose the most suitable data for fitting with the experimental ones. The obtained data for the polymer PM-555 are given in Tables I and II showing a good agreement with the theoretical work of G. Almasi et al. [8]. On the other hand, Tables III and IV represent the obtained data for the metaphosphate glass which are the first data for this material. These data seem to have the same features of the track detectors and introduce a good basis for studying the metaphosphate glass as a nuclear track detector.

CONCLUSION

A new track registration criteria is presented. The most important features are:

- 1- The total rate of energy loss of a charged particle cannot be used to predict track registration.
- 2- The restricted energy loss, REL, of charged particles

has been found to accurately predict track registration in PM-555 and in metaphosphate glass ZnP nuclear track detectors. In order to produce a latent (etchable) track, a charged particle must have an REL above a critical value REL_{crit} , which is a characteristic of the recording material.

REFERENCES

- [1] S.A. Durrani, Nuclear Tracks 4, pp 209-228, 1982.
- [2] R.P. Henke and E.V. Benton, Charged Particle Tracks in Polymers, No. 5, "A Computer Code for the Computation of Heavy Ion Range-Energy Relationships in any Stopping Material", *US Naval Radiological Defence Laboratory, San Francisco, Report USNRDL-TR-67-122, 1968.*
- [3] W.H. Barakas and M.J. Berger, *National Academic Sciences-National Research Council Publication-1133*, p. 103, 1964.
- [4] R.P. Henke and E.V. Benton, *USNRDL-TR-122*, 1967.
- [5] E.V. Benton, *USNRDL-TR-86-14*, 1988.
- [6] G. Somogyi, K. Grabisch, R. Scherzer and W. Enge, *Nucl. Instr. Meth.*, vol. 134, p. 129, 1976.
- [7] S.A. Durrani and R.K. Bull, "Solid State Nuclear Track Detection: Principles, Methods, and Applications", *Pergamon Press, Oxford UK*, p. 162, 1986.
- [8] G. Almasi and G. Somogyi, "Range and REL Data for Light and Heavy Ions in CR-39, CN-85 and PC Nuclear Track Detectors", *Atomki Közlemenyek*, vol. 23, p. 99, 1981.

Energy/ nucl. (MeV/a.m.u.)	$\omega_0=100$ eV		$\omega_0=200$ eV		$\omega_0=300$ eV		$\omega_0=500$ eV		$\omega_0=1000$ eV	
	^1H	^4He	^1H	^4He	^1H	^4He	^1H	^4He	^1H	^4He
.0025	-2.33E+03	1.105E+03	5.828E+02	1.105E+03	5.828E+02	1.105E+03	5.828E+02	1.105E+03	5.828E+02	1.105E+03
.005	5.970E+02	1.343E+03	6.586E+02	1.343E+03	6.586E+02	1.343E+03	6.586E+02	1.343E+03	6.586E+02	1.343E+03
.0075	5.263E+02	1.503E+03	7.094E+02	1.503E+03	7.094E+02	1.503E+03	7.094E+02	1.503E+03	7.094E+02	1.503E+03
.01	5.196E+02	1.618E+03	7.450E+02	1.618E+03	7.450E+02	1.618E+03	7.450E+02	1.618E+03	7.450E+02	1.618E+03
.02	5.427E+02	1.885E+03	8.207E+02	1.885E+03	8.207E+02	1.885E+03	8.207E+02	1.885E+03	8.207E+02	1.885E+03
.03	5.601E+02	2.019E+03	8.526E+02	2.019E+03	8.526E+02	2.019E+03	8.526E+02	2.019E+03	8.526E+02	2.019E+03
.04	5.691E+02	2.096E+03	8.670E+02	2.096E+03	8.670E+02	2.096E+03	8.670E+02	2.096E+03	8.670E+02	2.096E+03
.05	5.509E+02	2.051E+03	8.723E+02	2.144E+03	8.723E+02	2.144E+03	8.723E+02	2.144E+03	8.723E+02	2.144E+03
.06	5.146E+02	1.916E+03	8.724E+02	2.173E+03	8.724E+02	2.173E+03	8.724E+02	2.173E+03	8.724E+02	2.173E+03
.07	4.875E+02	1.814E+03	8.691E+02	2.189E+03	8.691E+02	2.189E+03	8.691E+02	2.189E+03	8.691E+02	2.189E+03
.08	4.662E+02	1.732E+03	8.637E+02	2.197E+03	8.637E+02	2.197E+03	8.637E+02	2.197E+03	8.637E+02	2.197E+03
.09	4.489E+02	1.666E+03	8.569E+02	2.198E+03	8.569E+02	2.198E+03	8.569E+02	2.198E+03	8.569E+02	2.198E+03
.1	4.429E+02	1.610E+03	8.356E+02	2.126E+03	8.613E+02	2.195E+03	8.613E+02	2.195E+03	8.613E+02	2.195E+03
.2	2.801E+02	1.312E+03	5.235E+02	1.665E+03	5.907E+02	1.871E+03	6.537E+02	2.064E+03	6.537E+02	2.064E+03
.3	2.084E+02	1.164E+03	3.908E+02	1.434E+03	4.386E+02	1.592E+03	4.988E+02	1.790E+03	5.313E+02	1.897E+03
.4	1.688E+02	1.080E+03	3.176E+02	1.299E+03	3.546E+02	1.427E+03	4.012E+02	1.588E+03	4.525E+02	1.765E+03
.5	1.434E+02	9.390E+02	2.706E+02	1.123E+03	3.006E+02	1.230E+03	3.385E+02	1.365E+03	3.899E+02	1.549E+03
.6	1.255E+02	8.286E+02	2.373E+02	9.867E+02	2.626E+02	1.079E+03	2.945E+02	1.196E+03	3.378E+02	1.354E+03
.7	1.122E+02	7.410E+02	2.124E+02	8.797E+02	2.342E+02	9.609E+02	2.617E+02	1.063E+03	2.990E+02	1.202E+03
.8	1.018E+02	6.704E+02	1.928E+02	7.939E+02	2.120E+02	8.661E+02	2.361E+02	9.572E+02	2.689E+02	1.081E+03
.9	9.343E+01	6.151E+02	1.770E+02	7.263E+02	1.940E+02	7.914E+02	2.156E+02	8.733E+02	2.448E+02	9.846E+02
1	8.764E+01	5.688E+02	1.638E+02	6.699E+02	1.792E+02	7.290E+02	1.986E+02	8.035E+02	2.250E+02	9.047E+02
2	5.396E+01	3.507E+02	1.003E+02	4.032E+02	1.080E+02	4.339E+02	1.178E+02	4.726E+02	1.310E+02	5.251E+02
3	3.948E+01	2.577E+02	7.312E+01	2.930E+02	7.830E+01	3.136E+02	8.482E+01	3.396E+02	9.367E+01	3.750E+02
4	3.116E+01	2.038E+02	5.756E+01	2.304E+02	6.145E+01	2.459E+02	6.635E+01	2.655E+02	7.300E+01	2.921E+02
5	2.570E+01	1.682E+02	4.736E+01	1.895E+02	5.047E+01	2.019E+02	5.440E+01	2.176E+02	5.973E+01	2.389E+02
6	2.182E+01	1.436E+02	4.033E+01	1.613E+02	4.293E+01	1.717E+02	4.621E+01	1.849E+02	5.066E+01	2.026E+02
7	1.921E+01	1.269E+02	3.553E+01	1.421E+02	3.776E+01	1.511E+02	4.058E+01	1.623E+02	4.439E+01	1.776E+02
8	1.718E+01	1.138E+02	3.179E+01	1.272E+02	3.375E+01	1.350E+02	3.621E+01	1.448E+02	3.956E+01	1.582E+02
9	1.556E+01	1.033E+02	2.879E+01	1.152E+02	3.053E+01	1.221E+02	3.273E+01	1.309E+02	3.571E+01	1.428E+02
10	1.423E+01	9.459E+01	2.633E+01	1.053E+02	2.790E+01	1.116E+02	2.988E+01	1.195E+02	3.257E+01	1.303E+02
11	1.312E+01	8.733E+01	2.428E+01	9.711E+01	2.571E+01	1.028E+02	2.751E+01	1.100E+02	2.995E+01	1.198E+02
12	1.217E+01	8.116E+01	2.253E+01	9.014E+01	2.385E+01	9.539E+01	2.550E+01	1.020E+02	2.775E+01	1.110E+02
13	1.136E+01	7.586E+01	2.104E+01	8.415E+01	2.225E+01	8.901E+01	2.378E+01	9.512E+01	2.586E+01	1.034E+02
14	1.066E+01	7.124E+01	1.974E+01	7.895E+01	2.087E+01	8.347E+01	2.229E+01	8.916E+01	2.422E+01	9.688E+01
15	1.004E+01	6.718E+01	1.860E+01	7.440E+01	1.965E+01	7.862E+01	2.098E+01	8.393E+01	2.279E+01	9.115E+01
16	9.499E+00	6.359E+01	1.759E+01	7.037E+01	1.858E+01	7.433E+01	1.983E+01	7.932E+01	2.153E+01	8.610E+01
17	9.014E+00	6.039E+01	1.669E+01	6.678E+01	1.763E+01	7.051E+01	1.881E+01	7.522E+01	2.040E+01	8.161E+01
18	8.580E+00	5.752E+01	1.589E+01	6.356E+01	1.677E+01	6.710E+01	1.789E+01	7.155E+01	1.940E+01	7.759E+01
19	8.189E+00	5.493E+01	1.517E+01	6.066E+01	1.600E+01	6.402E+01	1.706E+01	6.824E+01	1.849E+01	7.398E+01
20	7.833E+00	5.258E+01	1.451E+01	5.804E+01	1.531E+01	6.123E+01	1.631E+01	6.525E+01	1.768E+01	7.070E+01

Table I. REL (MeV.cm².g) in PM-555, for ^1H and ^4He ions, Effect of ω_0 .

Energy/ nucl. (MeV/a.m.u.)	$\omega_0=100$ eV		$\omega_0=200$ eV		$\omega_0=300$ eV		$\omega_0=500$ eV		$\omega_0=1000$ eV	
	^{12}C	^{16}O	^{12}C	^{16}O	^{12}C	^{16}O	^{12}C	^{16}O	^{12}C	^{16}O
.0025	2.567E+03	3.022E+03	2.567E+03	3.022E+03	2.567E+03	3.022E+03	2.567E+03	3.022E+03	2.567E+03	3.022E+03
.005	3.287E+03	3.955E+03	3.287E+03	3.955E+03	3.287E+03	3.955E+03	3.287E+03	3.955E+03	3.287E+03	3.955E+03
.0075	3.756E+03	4.584E+03	3.756E+03	4.584E+03	3.756E+03	4.584E+03	3.756E+03	4.584E+03	3.756E+03	4.584E+03
.01	4.104E+03	5.063E+03	4.104E+03	5.063E+03	4.104E+03	5.063E+03	4.104E+03	5.063E+03	4.104E+03	5.063E+03
.02	4.956E+03	6.292E+03	4.956E+03	6.292E+03	4.956E+03	6.292E+03	4.956E+03	6.292E+03	4.956E+03	6.292E+03
.03	5.431E+03	7.025E+03	5.431E+03	7.025E+03	5.431E+03	7.025E+03	5.431E+03	7.025E+03	5.431E+03	7.025E+03
.04	6.070E+03	7.531E+03	6.070E+03	7.531E+03	6.070E+03	7.531E+03	6.070E+03	7.531E+03	6.070E+03	7.531E+03
.05	6.181E+03	7.535E+03	6.467E+03	7.906E+03	6.467E+03	7.906E+03	6.467E+03	7.906E+03	6.467E+03	7.906E+03
.06	5.968E+03	7.131E+03	6.785E+03	8.195E+03	6.785E+03	8.195E+03	6.785E+03	8.195E+03	6.785E+03	8.195E+03
.07	5.812E+03	7.278E+03	7.045E+03	8.893E+03	7.045E+03	8.893E+03	7.045E+03	8.893E+03	7.045E+03	8.893E+03
.08	5.694E+03	7.167E+03	7.262E+03	9.230E+03	7.262E+03	9.230E+03	7.262E+03	9.230E+03	7.262E+03	9.230E+03
.09	5.601E+03	7.087E+03	7.444E+03	9.522E+03	7.444E+03	9.522E+03	7.444E+03	9.522E+03	7.444E+03	9.522E+03
.1	5.527E+03	7.028E+03	7.353E+03	9.453E+03	7.598E+03	9.778E+03	7.598E+03	9.778E+03	7.598E+03	9.778E+03
.2	5.168E+03	6.864E+03	6.647E+03	8.893E+03	7.511E+03	1.008E+04	8.323E+03	1.119E+04	8.323E+03	1.119E+04
.3	4.973E+03	6.824E+03	6.238E+03	8.601E+03	6.978E+03	9.641E+03	7.911E+03	1.095E+04	8.413E+03	1.166E+04
.4	4.795E+03	6.746E+03	5.908E+03	8.340E+03	6.560E+03	9.272E+03	7.381E+03	1.045E+04	8.286E+03	1.174E+04
.5	4.619E+03	6.629E+03	5.617E+03	8.081E+03	6.202E+03	8.930E+03	6.938E+03	9.999E+03	7.938E+03	1.145E+04
.6	4.447E+03	6.488E+03	5.354E+03	7.823E+03	5.885E+03	8.605E+03	6.554E+03	9.589E+03	7.462E+03	1.093E+04
.7	4.281E+03	6.332E+03	5.113E+03	7.571E+03	5.600E+03	8.296E+03	6.214E+03	9.209E+03	7.047E+03	1.045E+04
.8	4.123E+03	6.169E+03	4.893E+03	7.326E+03	5.343E+03	8.003E+03	5.910E+03	8.856E+03	6.680E+03	1.001E+04
.9	3.974E+03	6.004E+03	4.690E+03	7.091E+03	5.108E+03	7.726E+03	5.636E+03	8.527E+03	6.352E+03	9.614E+03
1	3.833E+03	5.841E+03	4.502E+03	6.866E+03	4.894E+03	7.465E+03	5.387E+03	8.220E+03	6.057E+03	9.245E+03
2	2.898E+03	4.618E+03	3.305E+03	5.275E+03	3.543E+03	5.660E+03	3.843E+03	6.145E+03	4.251E+03	6.803E+03
3	2.300E+03	3.740E+03	2.592E+03	4.226E+03	2.763E+03	4.510E+03	2.978E+03	4.867E+03	3.270E+03	5.353E+03
4	1.888E+03	3.115E+03	2.115E+03	3.499E+03	2.248E+03	3.724E+03	2.415E+03	4.007E+03	2.642E+03	4.392E+03
5	1.552E+03	2.653E+03	1.737E+03	2.971E+03	1.845E+03	3.156E+03	1.982E+03	3.390E+03	2.167E+03	3.708E+03
6	1.318E+03	2.313E+03	1.474E+03	2.583E+03	1.565E+03	2.741E+03	1.680E+03	2.940E+03	1.837E+03	3.211E+03
7	1.158E+03	2.073E+03	1.293E+03	2.308E+03	1.372E+03	2.446E+03	1.471E+03	2.619E+03	1.607E+03	2.854E+03
8	1.033E+03	1.856E+03	1.152E+03	2.064E+03	1.222E+03	2.186E+03	1.309E+03	2.339E+03	1.428E+03	2.547E+03
9	9.364E+02	1.680E+03	1.043E+03	1.867E+03	1.105E+03	1.976E+03	1.183E+03	2.113E+03	1.289E+03	2.299E+03
10	8.562E+02	1.536E+03	9.522E+02	1.704E+03	1.008E+03	1.803E+03	1.079E+03	1.927E+03	1.175E+03	2.096E+03
11	7.895E+02	1.414E+03	8.770E+02	1.569E+03	9.282E+02	1.659E+03	9.927E+02	1.772E+03	1.080E+03	1.927E+03
12	7.330E+02	1.312E+03	8.134E+02	1.454E+03	8.605E+02	1.537E+03	9.198E+02	1.641E+03	1.000E+03	1.783E+03
13	6.845E+02	1.223E+03	7.590E+02	1.355E+03	8.025E+02	1.432E+03	8.574E+02	1.529E+03	9.319E+02	1.660E+03
14	6.425E+02	1.147E+03	7.118E+02	1.269E+03	7.523E+02	1.341E+03	8.034E+02	1.431E+03	8.727E+02	1.554E+03
15	6.056E+02	1.081E+03	6.705E+02	1.196E+03	7.084E+02	1.263E+03	7.561E+02	1.347E+03	8.210E+02	1.462E+03
16	5.731E+02	1.022E+03	6.340E+02	1.130E+03	6.696E+02	1.193E+03	7.145E+02	1.273E+03	7.754E+02	1.381E+03
17	5.441E+02	9.701E+02	6.015E+02	1.072E+03	6.351E+02	1.131E+03	6.774E+02	1.206E+03	7.349E+02	1.308E+03
18	5.182E+02	9.234E+02	5.725E+02	1.020E+03	6.042E+02	1.076E+03	6.443E+02	1.147E+03	6.986E+02	1.243E+03
19	4.947E+02	8.814E+02	5.463E+02	9.728E+02	5.764E+02	1.026E+03	6.144E+02	1.094E+03	6.660E+02	1.185E+03
20	4.735E+02	8.433E+02	5.226E+02	9.304E+02	5.513E+02	9.813E+02	5.874E+02	1.045E+03	6.365E+02	1.133E+03

Table II. REL (MeV.cm².g) in PM-555, for ^{12}C and ^{16}O ions, Effect of ω_0 .

Energy/ nucl. (MeV/a.m.u.)	$\omega_0=100$ eV		$\omega_0=200$ eV		$\omega_0=300$ eV		$\omega_0=500$ eV		$\omega_0=1000$ eV	
	^4He	^{12}C	^4He	^{12}C	^4He	^{12}C	^4He	^{12}C	^4He	^{12}C
.0025	8.769E+02	1.863E+03	8.769E+02	1.863E+03	8.833E+02	1.863E+03	8.769E+02	1.863E+03	8.769E+02	1.895E+03
.005	1.057E+03	2.384E+03	1.057E+03	2.384E+03	1.062E+03	2.384E+03	1.057E+03	2.384E+03	1.057E+03	2.423E+03
.0075	1.153E+03	2.709E+03	1.153E+03	2.709E+03	1.160E+03	2.709E+03	1.153E+03	2.709E+03	1.153E+03	2.754E+03
.01	1.212E+03	2.941E+03	1.212E+03	2.941E+03	1.222E+03	2.941E+03	1.212E+03	2.941E+03	1.212E+03	2.992E+03
.02	1.317E+03	3.484E+03	1.317E+03	3.484E+03	1.339E+03	3.484E+03	1.317E+03	3.484E+03	1.317E+03	3.551E+03
.03	1.357E+03	3.772E+03	1.357E+03	3.772E+03	1.386E+03	3.772E+03	1.357E+03	3.772E+03	1.357E+03	3.851E+03
.04	1.376E+03	4.179E+03	1.376E+03	4.179E+03	1.411E+03	4.179E+03	1.376E+03	4.179E+03	1.376E+03	4.271E+03
.05	1.301E+03	4.161E+03	1.386E+03	4.425E+03	1.424E+03	4.425E+03	1.386E+03	4.425E+03	1.386E+03	4.526E+03
.06	1.156E+03	3.869E+03	1.392E+03	4.621E+03	1.432E+03	4.621E+03	1.392E+03	4.621E+03	1.392E+03	4.730E+03
.07	1.049E+03	3.649E+03	1.394E+03	4.783E+03	1.436E+03	4.783E+03	1.394E+03	4.783E+03	1.394E+03	4.898E+03
.08	9.673E+02	3.476E+03	1.395E+03	4.919E+03	1.437E+03	4.919E+03	1.395E+03	4.919E+03	1.395E+03	5.038E+03
.09	9.037E+02	3.339E+03	1.394E+03	5.034E+03	1.436E+03	5.034E+03	1.394E+03	5.034E+03	1.394E+03	5.158E+03
.1	8.532E+02	3.228E+03	1.328E+03	4.909E+03	1.434E+03	5.134E+03	1.392E+03	5.134E+03	1.392E+03	5.260E+03
.2	6.511E+02	2.752E+03	9.754E+02	4.112E+03	1.204E+03	4.908E+03	1.343E+03	5.655E+03	1.343E+03	5.791E+03
.3	6.049E+02	2.635E+03	8.530E+02	3.799E+03	1.032E+03	4.480E+03	1.181E+03	5.338E+03	1.280E+03	5.931E+03
.4	5.985E+02	2.589E+03	7.995E+02	3.614E+03	9.458E+02	4.214E+03	1.065E+03	4.969E+03	1.229E+03	5.924E+03
.5	5.406E+02	2.556E+03	7.095E+02	3.475E+03	8.319E+02	4.013E+03	9.328E+02	4.690E+03	1.102E+03	5.724E+03
.6	4.914E+02	2.521E+03	6.369E+02	3.356E+03	7.418E+02	3.844E+03	8.292E+02	4.460E+03	9.748E+02	5.401E+03
.7	4.495E+02	2.480E+03	5.772E+02	3.246E+03	6.689E+02	3.694E+03	7.459E+02	4.259E+03	8.737E+02	5.124E+03
.8	4.135E+02	2.433E+03	5.271E+02	3.141E+03	6.086E+02	3.556E+03	6.774E+02	4.077E+03	7.911E+02	4.879E+03
.9	3.844E+02	2.382E+03	4.867E+02	3.040E+03	5.600E+02	3.426E+03	6.220E+02	3.911E+03	7.244E+02	4.657E+03
1	3.587E+02	2.326E+03	4.517E+02	2.942E+03	5.184E+02	3.303E+03	5.748E+02	3.757E+03	6.678E+02	4.455E+03
2	2.248E+02	1.843E+03	2.731E+02	2.218E+03	3.087E+02	2.437E+03	3.369E+02	2.713E+03	3.853E+02	3.146E+03
3	1.705E+02	1.528E+03	2.030E+02	1.797E+03	2.270E+02	1.954E+03	2.459E+02	2.152E+03	2.784E+02	2.461E+03
4	1.370E+02	1.283E+03	1.614E+02	1.492E+03	1.794E+02	1.614E+03	1.937E+02	1.768E+03	2.182E+02	2.007E+03
5	1.143E+02	1.064E+03	1.339E+02	1.234E+03	1.480E+02	1.334E+03	1.598E+02	1.460E+03	1.794E+02	1.652E+03
6	1.004E+02	9.272E+02	1.168E+02	1.071E+03	1.286E+02	1.155E+03	1.384E+02	1.261E+03	1.548E+02	1.423E+03
7	8.971E+01	8.220E+02	1.038E+02	9.463E+02	1.138E+02	1.019E+03	1.223E+02	1.111E+03	1.364E+02	1.250E+03
8	8.117E+01	7.388E+02	9.348E+01	8.483E+02	1.023E+02	9.123E+02	1.098E+02	9.930E+02	1.221E+02	1.116E+03
9	7.419E+01	6.742E+02	8.515E+01	7.720E+02	9.296E+01	8.292E+02	9.964E+01	9.013E+02	1.106E+02	1.010E+03
10	6.837E+01	6.199E+02	7.825E+01	7.082E+02	8.528E+01	7.599E+02	9.131E+01	8.250E+02	1.012E+02	9.235E+02
11	6.346E+01	5.743E+02	7.245E+01	6.548E+02	7.883E+01	7.020E+02	8.434E+01	7.614E+02	9.334E+01	8.510E+02
12	5.924E+01	5.354E+02	6.750E+01	6.095E+02	7.335E+01	6.528E+02	7.842E+01	7.074E+02	8.668E+01	7.897E+02
13	5.558E+01	5.019E+02	6.322E+01	5.704E+02	6.862E+01	6.105E+02	7.332E+01	6.610E+02	8.096E+01	7.371E+02
14	5.238E+01	4.727E+02	5.948E+01	5.365E+02	6.449E+01	5.738E+02	6.887E+01	6.208E+02	7.598E+01	6.915E+02
15	4.956E+01	4.469E+02	5.620E+01	5.066E+02	6.087E+01	5.415E+02	6.497E+01	5.854E+02	7.161E+01	6.515E+02
16	4.704E+01	4.241E+02	5.328E+01	4.801E+02	5.766E+01	5.129E+02	6.152E+01	5.542E+02	6.775E+01	6.161E+02
17	4.479E+01	4.037E+02	5.067E+01	4.565E+02	5.479E+01	4.874E+02	5.844E+01	5.263E+02	6.431E+01	5.847E+02
18	4.276E+01	3.853E+02	4.832E+01	4.352E+02	5.222E+01	4.645E+02	5.567E+01	5.013E+02	6.123E+01	5.565E+02
19	4.092E+01	3.686E+02	4.620E+01	4.161E+02	4.989E+01	4.438E+02	5.317E+01	4.788E+02	5.845E+01	5.311E+02
20	3.925E+01	3.535E+02	4.427E+01	3.987E+02	4.778E+01	4.251E+02	5.090E+01	4.583E+02	5.593E+01	5.081E+02

Table III. REL (MeV.cm².g) in Zn_p, for ^4He and ^{12}C ions, Effect of ω_0 .

Energy/nucleon (MeV/a.m.u.)	$\omega_0=100$ eV		$\omega_0=200$ eV		$\omega_0=300$ eV		$\omega_0=500$ eV		$\omega_0=1000$ eV	
	^{16}O	^{238}U	^{16}O	^{238}U	^{16}O	^{238}U	^{16}O	^{238}U	^{16}O	^{238}U
.0025	2.171E+03	5.803E+03	2.171E+03	5.803E+03	2.171E+03	5.803E+03	2.171E+03	5.803E+03	2.171E+03	5.803E+03
.005	2.842E+03	8.149E+03	2.842E+03	8.149E+03	2.842E+03	8.149E+03	2.842E+03	8.149E+03	2.842E+03	8.149E+03
.0075	3.282E+03	9.925E+03	3.282E+03	9.925E+03	3.282E+03	9.925E+03	3.282E+03	9.925E+03	3.282E+03	9.925E+03
.01	3.609E+03	1.141E+04	3.609E+03	1.141E+04	3.609E+03	1.141E+04	3.609E+03	1.141E+04	3.609E+03	1.141E+04
.02	4.426E+03	1.590E+04	4.426E+03	1.590E+04	4.426E+03	1.590E+04	4.426E+03	1.590E+04	4.426E+03	1.590E+04
.03	4.899E+03	1.926E+04	4.899E+03	1.926E+04	4.899E+03	1.926E+04	4.899E+03	1.926E+04	4.899E+03	1.926E+04
.04	5.221E+03	2.204E+04	5.221E+03	2.204E+04	5.221E+03	2.204E+04	5.221E+03	2.204E+04	5.221E+03	2.204E+04
.05	5.118E+03	2.219E+04	5.459E+03	2.444E+04	5.459E+03	2.444E+04	5.459E+03	2.444E+04	5.459E+03	2.444E+04
.06	4.663E+03	1.995E+04	5.642E+03	2.658E+04	5.642E+03	2.658E+04	5.642E+03	2.658E+04	5.642E+03	2.658E+04
.07	4.616E+03	1.823E+04	6.102E+03	2.851E+04	6.102E+03	2.851E+04	6.102E+03	2.851E+04	6.102E+03	2.851E+04
.08	4.424E+03	1.689E+04	6.322E+03	3.029E+04	6.322E+03	3.029E+04	6.322E+03	3.029E+04	6.322E+03	3.029E+04
.09	4.273E+03	1.582E+04	6.514E+03	3.194E+04	6.514E+03	3.194E+04	6.514E+03	3.194E+04	6.514E+03	3.194E+04
.1	4.152E+03	1.495E+04	6.384E+03	3.129E+04	6.683E+03	3.348E+04	6.683E+03	3.348E+04	6.683E+03	3.348E+04
.2	3.689E+03	1.172E+04	5.555E+03	2.745E+04	6.648E+03	3.666E+04	7.672E+03	4.530E+04	7.672E+03	4.530E+04
.3	3.629E+03	1.207E+04	5.264E+03	2.736E+04	6.220E+03	3.630E+04	7.426E+03	4.756E+04	8.075E+03	5.363E+04
.4	3.635E+03	1.343E+04	5.102E+03	2.835E+04	5.960E+03	3.708E+04	7.041E+03	4.807E+04	8.232E+03	6.019E+04
.5	3.644E+03	1.515E+04	4.979E+03	2.975E+04	5.760E+03	3.829E+04	6.745E+03	4.906E+04	8.081E+03	6.367E+04
.6	3.639E+03	1.697E+04	4.868E+03	3.130E+04	5.587E+03	3.968E+04	6.493E+03	5.024E+04	7.723E+03	6.458E+04
.7	3.619E+03	1.881E+04	4.759E+03	3.289E+04	5.426E+03	4.112E+04	6.267E+03	5.150E+04	7.408E+03	6.558E+04
.8	3.584E+03	2.061E+04	4.649E+03	3.446E+04	5.272E+03	4.256E+04	6.057E+03	5.277E+04	7.122E+03	6.663E+04
.9	3.537E+03	2.235E+04	4.537E+03	3.599E+04	5.122E+03	4.397E+04	5.859E+03	5.402E+04	6.859E+03	6.767E+04
1	3.481E+03	2.401E+04	4.424E+03	3.746E+04	4.975E+03	4.532E+04	5.670E+03	5.523E+04	6.613E+03	6.869E+04
2	2.882E+03	3.690E+04	3.487E+03	4.889E+04	3.841E+03	5.591E+04	4.287E+03	6.474E+04	4.893E+03	7.674E+04
3	2.436E+03	4.490E+04	2.883E+03	5.590E+04	3.144E+03	6.234E+04	3.473E+03	7.045E+04	3.920E+03	8.145E+04
4	2.078E+03	4.981E+04	2.432E+03	6.005E+04	2.639E+03	6.604E+04	2.899E+03	7.359E+04	3.253E+03	8.384E+04
5	1.801E+03	5.274E+04	2.093E+03	6.237E+04	2.264E+03	6.800E+04	2.479E+03	7.510E+04	2.771E+03	8.473E+04
6	1.622E+03	5.474E+04	1.871E+03	6.385E+04	2.016E+03	6.918E+04	2.199E+03	7.590E+04	2.448E+03	8.502E+04
7	1.475E+03	5.589E+04	1.692E+03	6.456E+04	1.818E+03	6.963E+04	1.977E+03	7.602E+04	2.194E+03	8.469E+04
8	1.331E+03	5.644E+04	1.523E+03	6.472E+04	1.634E+03	6.956E+04	1.775E+03	7.567E+04	1.967E+03	8.395E+04
9	1.213E+03	6.091E+04	1.384E+03	6.884E+04	1.485E+03	7.348E+04	1.611E+03	7.933E+04	1.783E+03	8.727E+04
10	1.114E+03	6.156E+04	1.270E+03	6.918E+04	1.360E+03	7.364E+04	1.475E+03	7.926E+04	1.630E+03	8.689E+04
11	1.031E+03	6.182E+04	1.173E+03	6.917E+04	1.256E+03	7.346E+04	1.360E+03	7.887E+04	1.502E+03	8.622E+04
12	9.597E+02	6.178E+04	1.090E+03	6.887E+04	1.167E+03	7.302E+04	1.263E+03	7.824E+04	1.394E+03	8.533E+04
13	8.981E+02	6.151E+04	1.019E+03	6.837E+04	1.090E+03	7.238E+04	1.179E+03	7.743E+04	1.300E+03	8.428E+04
14	8.443E+02	6.107E+04	9.570E+02	6.771E+04	1.023E+03	7.159E+04	1.106E+03	7.648E+04	1.219E+03	8.312E+04
15	7.985E+02	6.050E+04	9.041E+02	6.693E+04	9.658E+02	7.070E+04	1.044E+03	7.544E+04	1.149E+03	8.188E+04
16	7.571E+02	5.982E+04	8.563E+02	6.607E+04	9.144E+02	6.973E+04	9.875E+02	7.434E+04	1.087E+03	8.059E+04
17	7.202E+02	5.908E+04	8.138E+02	6.516E+04	8.685E+02	6.871E+04	9.375E+02	7.319E+04	1.031E+03	7.927E+04
18	6.870E+02	5.828E+04	7.756E+02	6.420E+04	8.275E+02	6.766E+04	8.928E+02	7.201E+04	9.814E+02	7.793E+04
19	6.571E+02	5.745E+04	7.412E+02	6.321E+04	7.904E+02	6.658E+04	8.524E+02	7.083E+04	9.366E+02	7.659E+04
20	6.299E+02	5.660E+04	7.100E+02	6.221E+04	7.568E+02	6.550E+04	8.159E+02	6.964E+04	8.960E+02	7.526E+04

Table IV. REL (MeV.cm².g) in ZnP, for ^{16}O and ^{238}U ions, Effect of ω_0 .